nature chemistry

ARTICLES

https://doi.org/10.1038/s41557-022-00974-5

Check for updates

Sustainable polyesters via direct functionalization of lignocellulosic sugars

Lorenz P. Manker[1], Graham R. Dick[1], Adrien Demongeot[2], Maxime A. Hedou[1], Christèle Rayroud[1], Thibault Rambert[1], Marie J. Jones[1,3], Irina Sulaeva[4,5], Mariella Vieli[1], Yves Leterrier[2], Antje Potthast[4], François Maréchal[3], Véronique Michaud[2], Harm-Anton Klok[6] and Jeremy S. Luterbacher[1]✉

The development of sustainable plastics from abundant renewable feedstocks has been limited by the complexity and efficiency of their production, as well as their lack of competitive material properties. Here we demonstrate the direct transformation of the hemicellulosic fraction of non-edible biomass into a tricyclic diester plastic precursor at 83% yield (95% from commercial xylose) during integrated plant fractionation with glyoxylic acid. Melt polycondensation of the resulting diester with a range of aliphatic diols led to amorphous polyesters (M_n = 30–60 kDa) with high glass transition temperatures (72–100 °C), tough mechanical properties (ultimate tensile strengths of 63–77 MPa, tensile moduli of 2,000–2,500 MPa and elongations at break of 50–80%) and strong gas barriers (oxygen transmission rates (100 μm) of 11–24 cc m^{-2} day^{-1} bar^{-1} and water vapour transmission rates (100 μm) of 25–36 g m^{-2} day^{-1}) that could be processed by injection moulding, thermoforming, twin-screw extrusion and three-dimensional printing. Although standardized biodegradation studies still need to be performed, the inherently degradable nature of these materials facilitated their chemical recycling via methanolysis at 64 °C, and eventual depolymerization in room-temperature water.

Recyclable or biodegradable biomass-derived polymers could facilitate our economies' decoupling from fossil resources and prevent the accumulation of plastics in the environment[1]. However, producing these plastics from biomass at costs that are competitive with their fossil counterparts while achieving comparable or improved material properties—namely thermal stability, mechanical strength, processability and compatibility—has proven challenging[2,3]. Currently, most commercial bioplastics rely on efficient biological cultivation from edible sugars (for example, poly(lactic acid) (PLA), poly(hydroxyalkanoate)s (PHAs) and poly(butylene succinate) (PBS)), but elegant synthetic routes to renewable PHAs have now also been developed[4,5]. These industrial biological cultivations generally constrain monomer production to linear aliphatic diacids, diols and hydroxy acids, which has so far led to useful crystalline bioplastics, but that generally suffer from low glass transition temperatures (T_g), poor ductility or high gas permeability[6]. Combined with the high production costs from renewable resources, the lack of well-rounded or performance-advantaged material properties in these current commercial bioplastics has made it difficult to replace many petroleum-based alternatives in a very competitive industry.

Alternatively, chemical sugar transformations can be used to access molecules with improved structure and notably rigid cyclic molecules that can increase T_g and lower gas permeability[7,8]. A challenge in this approach is the ease with which these molecules can be accessed from abundant renewable substrates in terms of the number of reaction steps, costs of reagents and catalysts, and the complexity of the overall processes. The industrial production of 2,5-furandicarboxylic acid (FDCA), a prominent cyclic bio-based monomer, currently relies on edible sugars, and requires a dehydration step and a metal-catalysed oxidation step[9]. From lignocellulosic biomass the process is more complex, as it typically involves depolymerization to glucose, isomerization to fructose, dehydration to hydroxymethylfurfural (or its ethers) and a metal-catalysed oxidation[10]. Although feasible, this process complexity has limited the overall yields from cellulose and increased the separation costs, which has been a challenge for the production of lignocellulose-derived poly(ethylene furandicarboxylate) (PEF). To increase the likelihood of bringing more sustainable and performance-advantaged polymers to market alongside PEF, monomers that exploit the inherent cyclic structures of biomass with few chemical transformations and purification steps should be targeted.

Currently, the sugars required for both biological cultivations and chemical processes are usually extracted from edible biomass, but ideally these would be produced by depolymerization of the structural carbohydrates of lignocellulosic biomass. Cellulose and hemicellulose are more abundant, can be grown on marginal lands, and their simple sugars are projected to be far less expensive and more sustainable compared to their edible counterparts[11,12]. However, their industrial use has been limited by the high cost of their saccharification and subsequent fermentation, and the lack

[1]Laboratory of Sustainable and Catalytic Processing (LPDC), Institute of Chemical Sciences and Engineering (ISIC), School of Basic Sciences (SB), École Polytechnique Fédérale de Lausanne (EPFL), Lausanne, Switzerland. [2]Laboratory for Processing of Advanced Composites (LPAC), Institute of Materials (IMX), School of Engineering (STI), École Polytechnique Fédérale de Lausanne (EPFL), Lausanne, Switzerland. [3]Industrial Process and Energy Systems Engineering (IPESE), École Polytechnique Fédérale de Lausanne (EPFL); EPFL Valais-Wallis, Sion, Switzerland. [4]Institute for Chemistry of Renewable Resources, Department of Chemistry, University of Natural Resources and Life Sciences, Vienna, Austria. [5]Wood K Plus – Competence Center for Wood Composites & Wood Chemistry, Kompetenzzentrum Holz GmbH, Linz, Austria. [6]Institut des Matériaux and Institut des Sciences et Ingénierie Chimiques, Laboratoire des Polymères, École Polytechnique Fédérale de Lausanne (EPFL), Lausanne, Switzerland. ✉e-mail: jeremy.luterbacher@epfl.ch

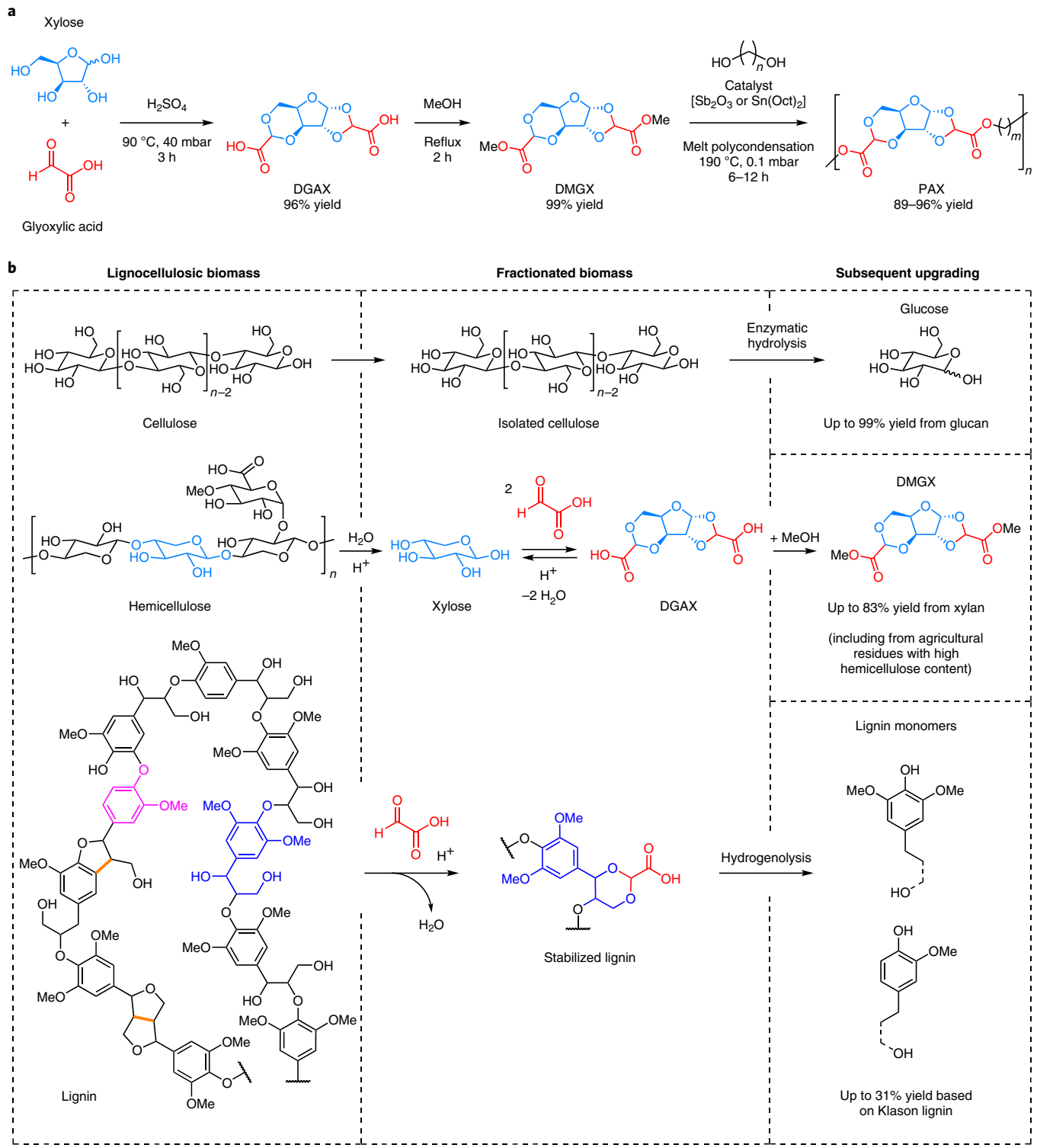

Fig. 1 | Production of PAX polyesters directly from xylose or during integrated lignocellulosic biomass fractionation. a, Direct production of DGAX from xylose, esterification to DMGX and polymerization to PAX. **b**, Production of DMGX via aldehyde-assisted fractionation of biomass followed by esterification with methanol. Both glyoxylic acid-stabilized lignin and cellulose-rich solids are also produced during fractionation and can be depolymerized to monomers. Glyoxylic acid prevents condensation of lignin and dehydration of xylose. The yields listed in the figure represent maximum product yields for each fraction, and not yields from a unique process (Fig. 2). As a benchmark for lignin yields[19], reductive catalytic fractionation of the same biomass resulted in a 56% yield of lignin monomers based on Klason lignin (see Supplementary Section 1.7.9 for an explanation of Klason lignin and Supplementary Table 7 for direct hydrogenolysis data).

of mature integrated lignocellulosic conversion processes that can valorize the non-polysaccharide fractions of the plant, which notably include lignin (15–30 wt/wt% of lignocellulosic biomass). Promising bioplastics from non-carbohydrate plant fractions such as plant oils[13] or lignin[14] are emerging, but they are inherently limited by their lower natural abundance or, in the case of lignin, the

lack of mature upgrading technologies, which makes achieving cost-competitiveness even more challenging than with sugars.

Accordingly, producing inexpensive sustainable bioplastics with attractive structural and end-of-life properties will probably depend on developing simple and direct high-yielding routes from abundant renewable resources. Ideally, these chemistries should aim to largely conserve the inherent structures in the feedstock, not only to reduce process complexity, but also to leverage any performance advantages that the chemical functionalities of the feedstock may provide[15]. Largely retaining the carbohydrate heterocycle in the final product structure could provide the required structural rigidity for both high T_g and strong barrier properties, while at the same time ensuring high atom economy and limiting the number of reactions. Recently, we developed a strategy that uses aldehydes to stabilize reactive intermediates during the fractionation of lignocellulosic biomass into an uncondensed, bench-stable, acetal-stabilized lignin, highly digestible, cellulose-rich solids and acetal-stabilized xyloses[16–18]. In this Article we show that, by using aldehydes with a secondary functionality, we can not only stabilize the hemicellulose-derived xylose and lignin, but can also directly produce fused, heterotricyclic, difunctional monomers with unique characteristics for bioplastic production. Specifically, we demonstrate the use of a carboxylic acid-functionalized aldehyde (glyoxylic acid) to produce a diacid precursor, diglyoxylic acid xylose (DGAX), and the corresponding diester, dimethylglyoxylate xylose (DMGX), directly from both xylose and lignocellulosic biomass, at high yield and using scalable processes (Fig. 1). Polymerizing DMGX with a range of diols produced a family of polyesters, hereafter referred to as poly(alkylene xylosediglyoxylates) (PAX), that are bio-based, degradable in water and chemically recyclable with combined high T_g, tough mechanical properties, strong gas barrier properties and straightforward processability.

Results and discussion

We have developed a one-pot, two-stage process for producing DMGX from commercial xylose in ≥95% overall yield (Supplementary Section 1.7.1 and Extended Data Fig. 1). Xylose and an excess of glyoxylic acid are heated in a melt in the presence of sulfuric acid to yield DGAX as a mixture of 4-stereoisomers (96% yield) at a concentration of 54 wt% in the crude reaction mixture. DMGX is then produced by adding methanol under reflux (99% yield with a crude concentration of 21 wt%) and purified by distillation and recrystallization (Extended Data Figs. 2 and 3), or by direct precipitation from the reaction mixture (Supplementary Section 1.7.5 and Extended Data Fig. 4). Notably, single stereoisomers can also be chirally resolved by stepwise crystallization (Supplementary Section 1.7.4).

To produce DMGX from lignocellulosic biomass, aldehyde-assisted fractionation[16,17] using glyoxylic acid is used to separate the biomass into its three principal components. Specifically, birch wood was treated with glyoxylic acid and a strong acid (H_2SO_4 or HCl), optionally in dioxane. After filtering off the cellulose-rich solids and precipitating the glyoxylic acid-stabilized lignin (Supplementary Fig. 1), DMGX was synthesized and purified from the remaining liquor as described for commercial xylose (Supplementary Sections 1.7.6–1.7.8 and Extended Data Fig. 5). Separately, the cellulose and lignin were depolymerized by enzymatic hydrolysis and hydrogenolysis, respectively, to determine the monomer yields that can be produced from these fractions (Supplementary Tables 1 and 2). We present three fractionation conditions: the first maximizes the yields of all three components (Fig. 2a; detailed mass balances are provided in Supplementary Fig. 2), the second maximizes DMGX yields (Fig. 2b), and the third maximizes lignin monomers (Fig. 2c). These strategies illustrate potential tradeoffs, but also opportunities to incorporate PAX production into an integrated biorefinery. The most favourable process would need to be selected for a particular biorefinery depending on local variables, such as location, feedstock and market demand. Notably, producing DMGX directly from a biomass-derived liquor did not increase the number of separation steps required to achieve a polymerizable product. This is noteworthy, because additional purification when using real plant-derived streams is often a major contributor to increased costs, and the associated greenhouse gas emissions, of bio-derived products[20].

Although we used birch wood for the preliminary studies, certain abundant and inexpensive agricultural wastes with high hemicellulose and low lignin content (for example, corn cobs, with ~30% hemicellulose)[21] would be ideal feedstocks for low-cost DMGX production. As a demonstration, we were able to produce DMGX in a one-pot process directly from raw corn cobs (not dried or pre-extracted) that contained 28 wt% hemicellulose (30 wt% xylose when hydrolysed) at 83% of theoretical yield (Supplementary Section 1.7.17). This translates to 25 wt% of the raw, non-edible waste biomass being directly incorporated into the DMGX plastic precursor. Utilization of waste biomass could provide a low-cost feedstock for DMGX production and could also ameliorate air quality and emissions issues in countries where crop waste is routinely burned, as it cannot be efficiently valorized[22].

When starting from either xylose or lignocellulosic biomass, the process is simple and scalable, uses an inexpensive mineral acid as the catalyst, and does not necessarily require a solvent. Glyoxylic acid is an inexpensive industrially available chemical (approximately US$1 kg^{-1}, Supplementary Section 2.1) that can be produced renewably either by oxidation of bio-derived ethylene glycol or ethanol[23] or by electrochemical reduction of oxalic acid produced from CO_2 (refs. [24,25]). Avantium and partners have already launched the OCEAN project, which aims to produce oxalic acid (and glyoxylic acid) from CO_2 at demonstration scale[26]. If this venture is successful, DMGX could be synthesized solely using carbon from CO_2 and non-edible biomass. A technoeconomic analysis of the production of high-purity (99.9%) crystalline DMGX (180 kt per annum) from commercial xylose (priced at US$1 kg^{-1}) estimated a minimum DMGX selling price of US$1,543 t^{-1} (Supplementary Section 2.1 and Extended Data Fig. 6). The major cost driver of the process is the price of xylose and glyoxylic acid, accounting for 78% of the total operating costs (35% and 43%, respectively). This scenario probably represents an upper bound of production costs, given that sugars from a biorefinery, or from agricultural residues, are projected to be substantially less expensive than current commercial xylose (that is, less than US$0.44 kg^{-1})[27]. This price for DMGX, at this scale, is almost within the market price range of purified terephthalic acid (~US$800–1,500 t^{-1})[28,29] and is below the market price range of PLA-grade lactic acid (~US$1,900–2,300 t^{-1})[20].

A cradle-to-gate life-cycle analysis of the simulated plant revealed a greenhouse warming potential (GWP) of 2.33 kg CO_2

Fig. 2 | Sankey diagram of the fractionation of birch wood with glyoxylic acid and the subsequent depolymerization and upgrading of the polysaccharide and lignin fractions. a, Fractionation using sulfuric acid in dioxane (13 wt% birch wood, 7 wt% glyoxylic acid, 3 wt% H_2SO_4, 3 wt% water and 74 wt% dioxane at 60 °C for 48 h). **b**, Fractionation using sulfuric acid in neat glyoxylic acid (13 wt% birch wood, 68 wt% glyoxylic acid, 2 wt% H_2SO_4 and 17 wt% water at 110 °C for 2 h 15 min). **c**, Fractionation using hydrochloric acid in dioxane (13 wt% birch wood, 7 wt% glyoxylic acid, 1 wt% HCl, 4 wt% water and 75 wt% dioxane at 60 °C for 24 h). The weight percentages of the sugars, DMGX, furfural, hydroxymethylfurfural (HMF), stabilized lignin and lignin monomers have been corrected to match their constituent masses as part of the native biomass. The arrow widths are proportional to the corresponding molar yields.

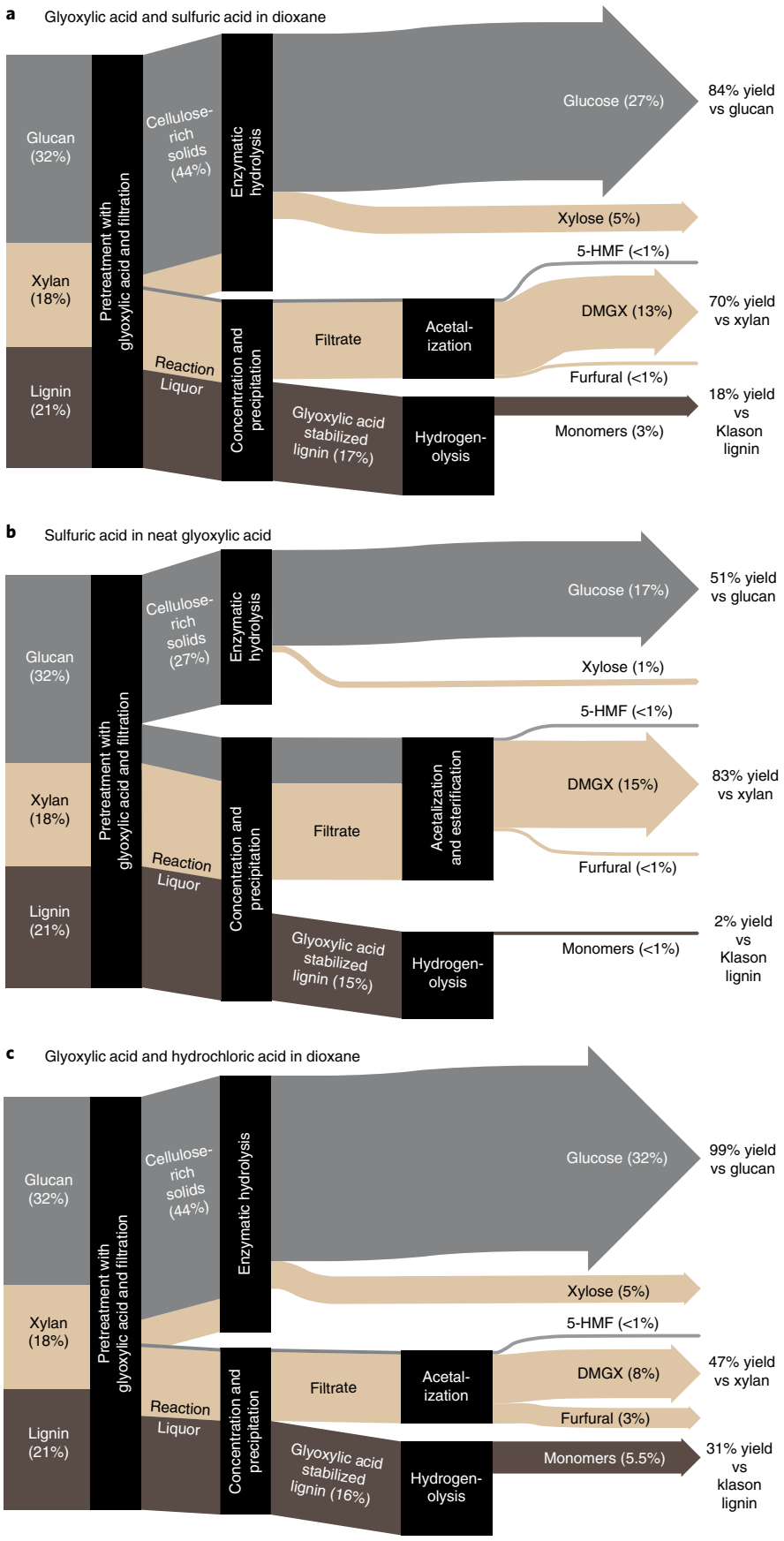
a
Glyoxylic acid and sulfuric acid in dioxane
Glucan (32%)
Xylan (18%)
Lignin (21%)
Pretreatment with glyoxylic acid and filtration
Cellulose-rich solids (44%)
Reaction Liquor
Enzymatic hydrolysis
Concentration and precipitation
Filtrate
Glyoxylic acid stabilized lignin (17%)
Acetal-ization
Hydrogen-olysis
Glucose (27%)
Xylose (5%)
5-HMF (<1%)
DMGX (13%)
Furfural (<1%)
Monomers (3%)
84% yield vs glucan
70% yield vs xylan
18% yield vs Klason lignin
b
Sulfuric acid in neat glyoxylic acid
Glucan (32%)
Xylan (18%)
Lignin (21%)
Pretreatment with glyoxylic acid and filtration
Cellulose-rich solids (27%)
Reaction Liquor
Enzymatic hydrolysis
Concentration and precipitation
Filtrate
Glyoxylic acid stabilized lignin (15%)
Acetalization and esterification
Hydrogen-olysis
Glucose (17%)
Xylose (1%)
5-HMF (<1%)
DMGX (15%)
Furfural (<1%)
Monomers (<1%)
51% yield vs glucan
83% yield vs xylan
2% yield vs Klason lignin
c
Glyoxylic acid and hydrochloric acid in dioxane
Glucan (32%)
Xylan (18%)
Lignin (21%)
Pretreatment with glyoxylic acid and filtration
Cellulose-rich solids (44%)
Reaction Liquor
Enzymatic hydrolysis
Concentration and precipitation
Filtrate
Glyoxylic acid stabilized lignin (16%)
Acetal-ization
Hydrogen-olysis
Glucose (32%)
Xylose (5%)
5-HMF (<1%)
DMGX (8%)
Furfural (3%)
Monomers (5.5%)
99% yield vs glucan
47% yield vs xylan
31% yield vs klason lignin

equivalent (CO_2e) per kg DMGX, which is 20% lower than our calculated GWP of terephthalic acid when using petroleum-based glyoxylic acid, xylose derived from viscose production (a common current source) and natural gas for steam and power production (Supplementary Section 2.2 provides a detailed description of the life-cycle analysis; Extended Data Fig. 7). In this case, 64% of the calculated GWP of DMGX was associated with the production of glyoxylic acid. If glyoxylic acid was instead sourced from CO_2, which may soon be feasible, DMGX production is estimated to have 71% lower associated emissions as compared to terephthalic acid (GWP of 0.8 kg CO_2e per kg DMGX). This could be further reduced to 15% of terephthalic acid's GWP if agricultural residues were used for heat production as opposed to natural gas, which is typical in a biorefinery.

Xylose-derived DMGX (distilled 4-stereoisomer oil; Extended Data Fig. 2 provides a full characterization) was polymerized with a range of aliphatic diols (C_2–C_6) via melt condensation to produce amorphous polyesters (89–96% yield). All polymerizations were conducted via transesterification of >99% pure DMGX (by gas chromatography; Supplementary Section 1.8.2) with excess diol and a Lewis acid catalyst with a final reaction temperature of 190–200 °C and 0.1 mbar of pressure. Reaction times differed slightly between diols, but the decreased volatility of the longer diols seemed to be compensated by the decrease in melt viscosity of the polymerization (increased mass transfer of the volatilized diol reaction by-product). Probably because of their high melt viscosities within the 190–200 °C temperature range, we were unable to obtain high-molecular-weight poly(ethylene xylosediglyoxylate) (PEX) and poly(propylene xylosediglyoxylate) (PPX). Both PEX and PPX were disperse and brittle and had number-averaged molecular weights (M_n) of 3 kDa and 8 kDa, respectively (Fig. 3a). However, plastics synthesized from more flexible diols (C_4–C_6) yielded polymers of $M_n \approx 35$ kDa with good dispersities (2.0–2.5) when using commercially relevant zinc acetate and antimony trioxide catalysts. As antimony trioxide is a suspected carcinogen, polymerization was also conducted with the potentially safer tin(II) 2-ethylhexanoate (TEH) catalyst to produce plastics with comparable properties (Supplementary Section 1.7.16). To explore the effect of molecular weight and stereochemistry on the polymer properties, higher-molecular-weight poly(pentylene xylosediglyoxylate) (HMW-PPTX, $M_n = 59$ kDa) and single DMGX stereoisomer (Extended Data Fig. 3 provides a complete characterization) poly(pentylene xylosediglyoxylate) (1S-PPTX, $M_n = 39$ kDa) were also synthesized. Finally, 1S-PPTX was also synthesized using DMGX produced from birch wood to confirm that true biomass-derived polymers could be synthesized without any substantial change in characteristics (Supplementary Section 1.7.12 and Extended Data Fig. 5). Matrix-assisted laser desorption/ionization time-of-flight mass spectroscopy (MALDI-TOF-MS; Supplementary Fig. 3) and two-dimensional (2D) heteronuclear single quantum coherence spectroscopy (HSQC; Supplementary Fig. 4) confirmed that all of the intended polymer structures were obtained with no evidence of polymerization by-products or acetal rupture.

Differential scanning calorimetry (DSC) and dynamic mechanical analysis (DMA; Extended Data Fig. 8) revealed a range of T_g from 72 °C for the poly(hexylene xylosediglyoxylate) (PHX) to 137 °C for PEX (Fig. 3b and Supplementary Table 3). The relatively high glass transition of these polyesters compared to commercial bioplastics and even PET (80 to 85 °C, 65 to 75 °C, 55 to 65 °C, −50 to −32 °C, and 5 °C for poly(ethylene furanote) (PEF), PET, PLA, PBS and poly(hydroxybutyrate) (PHB), respectively) is attributed to the rigid, tricyclic DMGX monomer. Unfortunately, the PEX polymer molecular weight was too low for processing and mechanical testing, as it was probably below its entanglement molecular weight. Also, because of the brittle nature of low-molecular-weight PPX, its mechanical properties could only be measured by DMA using thin films. Although PEX and PPX are currently too brittle to be mechanically useful, future increases in attainable molecular weights via optimized polymerization methods could allow us to exploit their high T_g values (which are only likely to increase with molecular weight). Poly(butylene xylosediglyoxylate) (PBX) is currently the PAX polymer with the highest glass transition temperature (100 °C) that is still easily processable. As a demonstration of its high glass transition, thin cups made from PBX were shown to retain their mechanical strength when exposed to boiling water, whereas cups made from PLA (or PET) will become soft and lose their form (Supplementary Fig. 5). The more ductile polymers, PPTX and PHX, have slightly lower glass transitions (84 °C and 74 °C), comparable to those of PEF and PET, respectively.

Neither DSC nor X-ray diffraction (XRD; Supplementary Fig. 6) showed evidence of crystalline phases in any of the DMGX polyesters, even for the polymer made from a single stereoisomer (1S-PPTX). The lack of crystallinity can be explained by the nonlinear, non-planar and asymmetric nature of DMGX (the crystal structure of an isomer is shown in Extended Data Fig. 3). These thermal characteristics enabled the processing of the PHX, PPTX and PBX polymers by common industrial techniques such as compression moulding (Fig. 3g), vacuum-forming (Fig. 3h), injection moulding (Fig. 3i) or combined twin-screw extrusion (Supplementary Fig. 5) and 3D printing (Fig. 3j) at temperatures as low as 140 °C and up to 200 °C (for extrusion of PBX). These are well below the degradation onset temperatures (319–344 °C) measured by thermogravimetric analysis (TGA; Extended Data Fig. 8). Notably, ^{1}H-NMR, HSQC and gel permeation chromatography (GPC) analysis of the PBX polymer ($M_n = 25$ kDa), before and after twin-screw extrusion and subsequent 3D printing (both at 200 °C and directly exposed to air), revealed a slight decrease in molecular weight (12.6% decrease in M_n), with no evident change in chemical structure, indicating that PAX polymers can withstand high-temperature, high-shear processing without substantial degradation or crosslinking (Supplementary Fig. 7). This stability under harsh processing conditions could potentially facilitate mechanical recycling of the polymer.

Tensile testing on injection-moulded dog bones revealed that PBX, PPTX and PHX were mechanically hard, strong and tough, with average tensile moduli of 2,000–2,500 MPa, ultimate tensile strengths of 63–70 MPa and elongations at break of 50–80% (Fig. 3c and Supplementary Table 3). Increasing the diol length led to increased ductility at the cost of lower tensile modulus and ultimate tensile strength. The high ductility of the PPTX and PHX polymers (4S and 1S) enabled cold-forming of fibres (Fig. 3e) and folding of thick samples without fracture (Supplementary Fig. 5). PBX was less ductile, and thicker samples would fracture under flexion. Notably, PAX tensile specimens exhibited post-yield necking and cold drawing followed by a period of strain hardening before ductile fracture (Extended Data Fig. 8, Supplementary Fig. 5 and Supplementary Video 1). Strain hardening was not observed in PPTX samples, probably because of premature fracture caused by slight defects in the tensile specimen. The degree of plasticity of these materials and their ability to strain harden is a useful parameter for stretch processing techniques (for example, blow moulding) and may facilitate their use in pressurized applications. The single stereoisomer PPTX polymer, 1S-PPTX, had a substantially improved ultimate tensile strength (77 MPa) when compared to PPTX (66 MPa) and demonstrated decreased melt viscosities (Supplementary Fig. 8), which facilitated thermal processing. Therefore, tuning the stereochemistry of PAX polymers could be used to control the polymer's performance. The presence of four DMGX stereoisomers and the ability to easily separate them by crystallization could lead to exciting opportunities for stereo-specific polymerization to high-performance block copolymers, as has already been shown in the literature for PHAs[5].

The measured oxygen transmission rates of films of PHX, PPTX and PBX were similar to those of PET[30], with slightly higher water

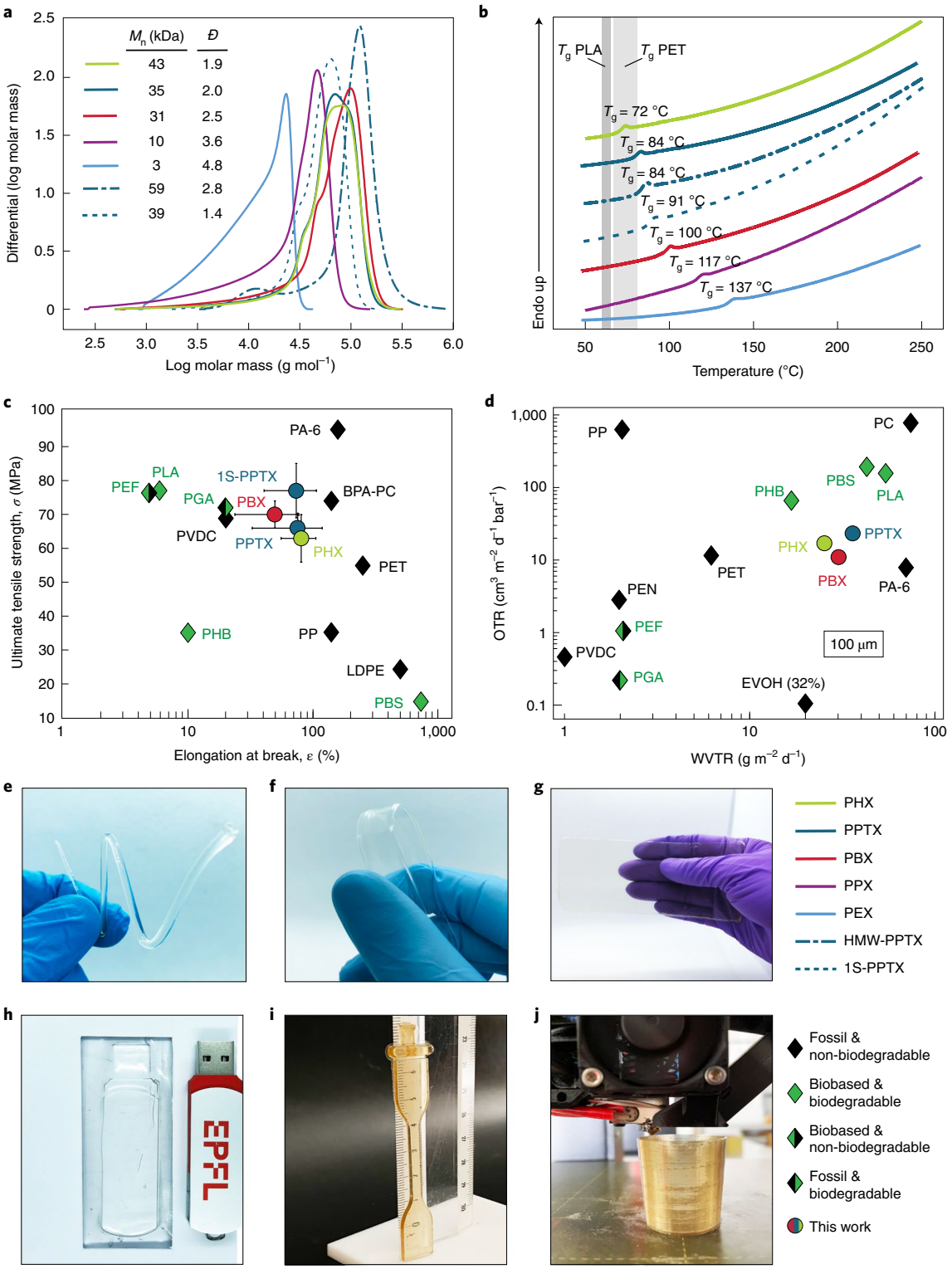

Fig. 3 | Properties of PAX polymers. a, Molecular weight distributions by GPC using triple detection. **b**, DSC curves at a heating rate of 10 °C min^{-1} under nitrogen. **c**, Average elongation at break versus average ultimate tensile strength for injection-moulded PAX and other commercial plastics from the literature (see Supplementary Table 4 for numerical tensile values and references, and Extended Data Fig. 8 for stress–strain curves). Error bars are standard errors from three to five samples. **d**, Water vapour transmission rate (WVTR; 37.8 °C, 90% relative humidity, 100 µm) versus oxygen transmission rate (OTR; 23 °C, 50% relative humidity, 1 bar, 100 µm) for PAX and other commercial plastics from the literature (Supplementary Table 5 provides numerical values and references). **e**,**f**, Fibre drawn quickly (**e**) and slowly (**f**), from molten 1S-PPTX using an optimized catalyst (TEH) and antioxidant (TTP) combination. **g**, Compression-moulded film of 1S-PPTX using DBTO as the catalyst with no antioxidant (thickness of 500 µm). **h**, Packaging for a USB key produced by vacuum-forming of PHX (thickness of 500 µm) produced with optimized catalyst and antioxidant. **i**, Injection-moulded dog bone using 1S-PPTX polymer and DBTO as the catalyst with no antioxidant. Ruler graduations are in centimetres. **j**, 3D-printed cup made using a twin-screw extruded PBX filament.

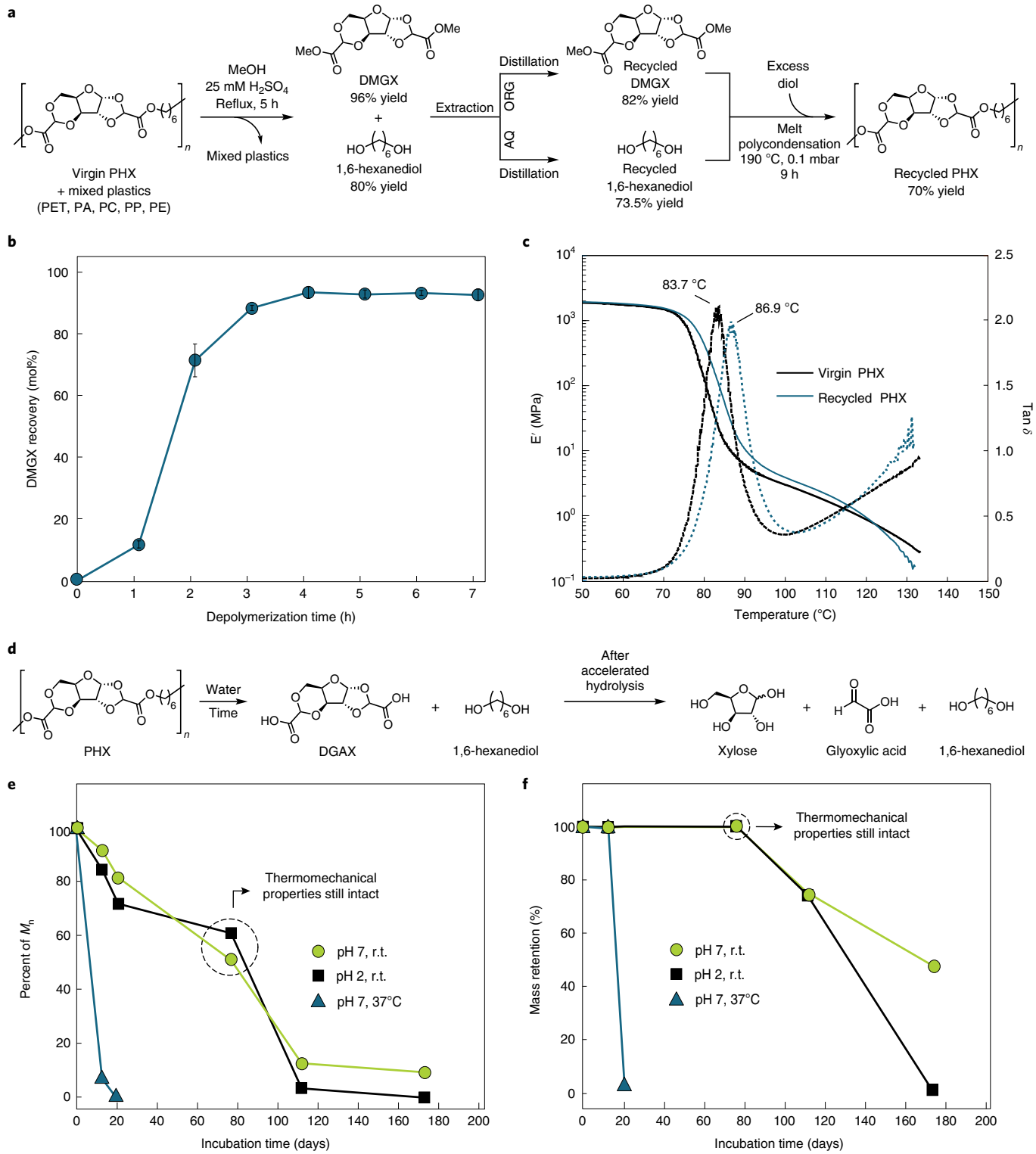

Fig. 4 | Chemical recycling and hydrolytic stability studies. a, Process schematic for chemical recycling of PHX from a mixed plastic stream (AQ, aqueous phase; ORG, organic phase). Yield of the recycled plastic from the mixed stream is based on DMGX utilization. **b**, DMGX recovery upon depolymerization of compression-moulded PHX in isolation (no mixed plastics) via alcoholysis in methanol under reflux with 25 mM sulfuric acid. Error bars are standard errors ($n = 3$). **c**, DMA curves of virgin and chemically recycled PHX from the mixed plastic waste stream (tanδ, loss tangent; E', storage modulus). The tanδ curves are shown as dashed lines. **d**, Schematic of PHX hydrolysis. PHX hydrolysed to DGAX and diol monomers in the extended hydrolytic studies at room temperature and 37 °C. Further hydrolysis of DGAX to xylose and glyoxylic acid occurred in the accelerated hydrolysis conditions (water at 100 °C). **e**, Percent of initial M_n as a function of incubation time of compression-moulded PHX samples (initial M_n of 43 kDa) immersed in buffered solutions at the indicated pH and temperature (r.t., room temperature). **f**, Mass retention of the plastic samples measured after removal from buffered solutions and thorough washing with deionized water then drying. Solid lines are guides to the eye and do not represent a model.

vapour transmission rates (Fig. 3d and Supplementary Table 3), potentially lending themselves to food packaging applications. The surprisingly low oxygen permeability of these amorphous polymers probably results from the polar and barrier-like nature of the rigid DMGX monomer, which may decrease oxygen solubility and diffusion, respectively. The slightly higher water vapour transmission rates, as compared to PET, are attributed to the hydrophilic nature of the DMGX monomer (greater water solubility).

PAX polymers derived from the distilled 4-stereoisomer DMGX oil were yellow in colour (Supplementary Fig. 9), which is undesirable in many applications and has been a substantial obstacle in the development of bio-based plastics such as PEF. Increasing the purity of the DMGX monomer by recrystallization resulted in plastics that could be processed into fibres and films with appreciably reduced colouration (Fig. 3g and Supplementary Fig. 5). The 4S-DMGX oil could be directly recrystallized as a mixture of four isomers to remove coloured impurities, or isomers could be partially resolved via stepwise crystallization (Supplementary Section 1.7.4). In thicker PAX samples, however, even the crystallized DMGX resulted in slight yellow colouration when zinc acetate or dibutyltin oxide (DBTO) were used as catalysts (Fig. 3i). Fortunately, initial tests indicate that optimized catalyst and antioxidant combinations can be used to dramatically reduce discolouring side reactions during polycondensation while maintaining similar reaction times (Supplementary Section 1.7.16). TEH (0.008 mol%) and triphenyl phosphite (TTP, 0.17 mol%) were used to produce near-colourless and transparent PHX products (Fig. 3e,f,h). DMA, GPC and TGA analysis of the polymers produced using TEH revealed similar molecular weights ($M_{n,TEH}$ = 21 kDa, $M_{n,DBTO}$ = 27 kDa) and thermomechanical properties (except for a slightly superior glass transition by onset of storage modulus decay and increased degradation onset temperature) as for those polymerized with the DBTO catalyst (Supplementary Fig. 10). Therefore, the impurities resulting in colouration of the PAX polymers produced with non-optimized catalysts do not appear to have any substantial impact on the final material properties (other than the increased colouration).

Chemical recycling of PAX, both in isolation and combined with a simulated mixed plastic waste stream, was demonstrated by alcoholysis (Fig. 4a–c and Supplementary Section 1.7.13). Compression-moulded PHX was fully depolymerized and solvated, with a 96% recovery of DMGX by refluxing in acidic methanol (25 mM H_2SO_4) for 4 h (Fig. 4b). The same yield was achieved from a simulated mixed plastic stream (Supplementary Fig. 5) containing commercial polyamide, polyethylene, polypropylene, polycarbonate and PET (used as received; Supplementary Sections 1.1 and 1.7.13.3 provide the plastic grades) in 5 h, without any evident contaminants from the non-PAX plastics (Supplementary Fig. 11). After filtering off the residual plastics (100% mass recovery of non-PAX plastics; Supplementary Fig. 5), the DMGX and 1,6-hexanediol were separated by liquid–liquid extraction and separately distilled to produce pure monomers in 82% and 74% yields, respectively (Extended Data Fig. 10 provides 2D NMR results for the recycled monomers). The reduced yields of purified DMGX result from separation losses at small scale in batch, and would probably be substantially improved in a large-scale, optimized, continuous process. PHX was then re-synthesized using the recycled monomers. HSQC (Extended Data Fig. 10) and DMA (Fig. 4c) revealed no notable change in chemical structure or thermomechanical properties between the virgin and recycled polymers. The slightly lower T_g of the virgin PHX was attributed to the removal of a polymerization antioxidant (Irganox 1010) during the chemical recycling process, demonstrating that the presence of polymerization additives will probably not hinder recyclability. Low-temperature methanolysis from a mixed plastic stream at atmospheric pressure using standard separation techniques (extraction and distillation or crystallization) may make industrial chemical recycling of PAX more economically feasible as compared to the high temperature and pressure operations required for less degradable plastics such as PET[31].

The easily depolymerizable nature of PAX polymers in alcoholytic conditions poses important questions regarding both the useful life of these materials and their physical and chemical fate, in the presence of water. In this context, hydrolytic stability tests were performed on compression-moulded samples of PHX (1.5 cm × 1.5 cm × 0.5 mm; Supplementary Fig. 9) with an initial M_n of 43 kDa over the course of 180 days under neutral and acidic conditions at room temperature, and under neutral conditions at 37 °C (Fig. 4d–f). After 77 days at room temperature for both the pH 2 and 7 solutions, the M_n declined to ~22 kDa (~55% of the initial M_n), with no mass loss. DMA analysis of these degraded samples revealed no notable change in thermomechanical properties compared to the original polymer, other than a slightly reduced melt strength (Supplementary Fig. 12). Following the 77-day timepoint, the plastics continued to hydrolyse and began to dissolve in the aqueous solutions. After 173 days in the pH 2 water, the plastic was essentially fully dissolved (<2% of initial mass remaining), but in the pH 7 water, 47 wt/wt% of the plastic remained with a reduced M_n of 4 kDa (9% of initial M_n). When the hydrolytic stability tests were performed at an elevated temperature of 37 °C at pH 7, the M_n declined to 3 kDa (7% of initial M_n) with no mass loss after 13 days, whereas after 20 days, the plastic was essentially fully dissolved (<4% of initial mass). The degraded plastic dissolved to a mixture of monomers (DGAX and 1,6-hexanediol) and oligomers (as determined by HPLC analysis; Supplementary Fig. 13). Hydrolytic degradation of identical films made from PLA (NatureWorks 4032D) revealed no observable mass loss or decrease in molecular weight by GPC over the 180-day experiment at room temperature. These results indicate that the degradation rates of PAX in water are substantially higher than those of current commercial polyesters, including degradable PLA. Although promising in terms of decreased plastic persistence, these properties may pose challenges in applications that require high hydrolytic stability.

To see whether hydrolytic stability would be augmented in other PAX polymers, hydrolytic stability tests were performed with PHX, PBX and 1S-PHX polymers with identical starting molecular weights ($M_n \approx 20$ kDa) at 37 °C. These tests revealed that the PBX and 1S-PHX polymers demonstrated a 30% and 90% increase in hydrolytic stability (incubation time with >99% mass retention) as compared to the PHX polymer, respectively (Extended Data Fig. 9). This indicates that PAX polymers made from a single stereoisomer, or polymers with higher T_g, could probably be used for products that require a longer shelf-life in aqueous environments. For applications in which hydrolytic cleavage rates need to be reduced even further, strategies including the use of anti-hydrolysis agents (for example, aromatic carbodiimides) have already been demonstrated to substantially increase the hydrolytic stability of degradable PLA and PGA, and could presumably be applied to PAX[32,33]. Importantly, under non-aqueous conditions, PAX polymers maintained ~74% of their initial molecular weight (43 kDa to 32 kDa) from synthesis, through thermal processing into a useful product, and a subsequent 18-month lifetime (Supplementary Section 2.3), indicating reasonable useful lifetimes if not continuously exposed to water. Short exposures to room temperature or boiling water did not visibly accelerate the degradation of PAX over its future lifetime (Supplementary Section 2.3 and Supplementary Fig. 14). Overall, the PAX polymers present as relatively degradable performance polyesters that could act as a complement to other less-degradable bio-based plastics such as PEF.

To gain preliminary insight into the long-term fate of PAX via simple hydrolysis, compression-moulded PHX was boiled in deuterium oxide (D_2O) and analysed by NMR over time. This study revealed depolymerization to diacid (DGAX) and 1,6-hexanediol after 9 h and subsequent partial hydrolysis of DGAX to glyoxylic

acid and xylose beginning after 17 h and continuing throughout the 120-h experiment (Supplementary Section 1.7.15 and Supplementary Figs. 15–17). These initial results suggest that the long-term fate of the polymer in water is likely to be hydrolysis to xylose, glyoxylic acid and diol, all of which are non-toxic and biodegradable[34–37]. However, DGAX is one of the primary hydrolysis products (along with the well-studied diol), and its toxicity and biodegradability are still unknown. Therefore, in-depth toxicological and biodegradation tests are still required before this polymer's environmental fate is fully understood. Nevertheless, this degradation pathway demonstrates that the preservation of the largely unmodified carbohydrate core, in addition to greatly facilitating the polyester's production and ensuring high atom economy, at the very least offers a hydrolytic route back to sugars.

Online content

Any methods, additional references, Nature Research reporting summaries, source data, extended data, supplementary information, acknowledgements, peer review information; details of author contributions and competing interests; and statements of data and code availability are available at https://doi.org/10.1038/s41557-022-00974-5.

Received: 21 October 2021; Accepted: 12 May 2022;
Published online: 23 June 2022

References

1. Geyer, R., Jambeck, J. R. & Law, K. L. Production, use and fate of all plastics ever made. *Sci. Adv.* **3**, e1700782 (2017).
2. Hillmyer, M. A. The promise of plastics from plants. *Science* **358**, 868–870 (2017).
3. Zhu, Y., Romain, C. & Williams, C. K. Sustainable polymers from renewable resources. *Nature* **540**, 354–362 (2016).
4. Tang, X. & Chen, E. Y.-X. Chemical synthesis of perfectly isotactic and high melting bacterial poly(3-hydroxybutyrate) from bio-sourced racemic cyclic diolide. *Nat. Commun.* **9**, 2345 (2018).
5. Tang, X., Westlie, A. H., Watson, E. M. & Chen, E. Y.-X. Stereosequenced crystalline polyhydroxyalkanoates from diastereomeric monomer mixtures. *Science* **366**, 754–758 (2019).
6. Wypych, G. *Handbook of Polymers* (Elsevier, 2016).
7. Rose, M. & Palkovits, R. Isosorbide as a renewable platform chemical for versatile applications—quo vadis? *ChemSusChem* **5**, 167–176 (2012).
8. Muñoz-Guerra, S., Lavilla, C., Japu, C. & Martínez de Ilarduya, A. Renewable terephthalate polyesters from carbohydrate-based bicyclic monomers. *Green Chem.* **16**, 1716–1739 (2014).
9. Stadler, B. M., Wulf, C., Werner, T., Tin, S. & de Vries, J. G. Catalytic approaches to monomers for polymers based on renewables. *ACS Catal.* **9**, 8012–8067 (2019).
10. Sajid, M., Zhao, X. & Liu, D. Production of 2,5-furandicarboxylic acid (FDCA) from 5-hydroxymethylfurfural (HMF): recent progress focusing on the chemical-catalytic routes. *Green Chem.* **20**, 5427–5453 (2018).
11. Shahzadi, T. et al. Advances in lignocellulosic biotechnology: a brief review on lignocellulosic biomass and cellulases. *Adv. Biosci. Biotechnol.* **05**, 246–251 (2014).
12. Naik, S. N., Goud, V. V., Rout, P. K. & Dalai, A. K. Production of first and second generation biofuels: a comprehensive review. *Renew. Sust. Energ. Rev.* **14**, 578–597 (2010).
13. Häußler, M., Eck, M., Rothauer, D. & Mecking, S. Closed-loop recycling of polyethylene-like materials. *Nature* **590**, 423–427 (2021).
14. Upton, B. M. & Kasko, A. M. Strategies for the conversion of lignin to high-value polymeric materials: review and perspective. *Chem. Rev.* **116**, 2275–2306 (2016).
15. Cywar, R. M., Rorrer, N. A., Hoyt, C. B., Beckham, G. T. & Chen, E. Y.-X. Bio-based polymers with performance-advantaged properties. *Nat. Rev. Mater.* **7**, 83–103 (2022).
16. Shuai, L. et al. Formaldehyde stabilization facilitates lignin monomer production during biomass depolymerization. *Science* **354**, 329–333 (2016).
17. Lan, W., Amiri, M. T., Hunston, C. M. & Luterbacher, J. S. Protection group effects during α,γ-diol lignin stabilization promote high-selectivity monomer production. *Angew. Chem. Int. Ed.* **57**, 1356–1360 (2018).
18. Questell-Santiago, Y. M., Zambrano-Varela, R., Talebi Amiri, M. & Luterbacher, J. S. Carbohydrate stabilization extends the kinetic limits of chemical polysaccharide depolymerization. *Nat. Chem.* **10**, 1222–1228 (2018).
19. Talebi Amiri, M., Dick, G. R., Questell-Santiago, Y. M. & Luterbacher, J. S. Fractionation of lignocellulosic biomass to produce uncondensed aldehyde-stabilized lignin. *Nat. Protoc.* **14**, 921–954 (2019).
20. Biddy, M. J., Scarlata, C. & Kinchin, C. *Chemicals from Biomass: A Market Assessment of Bioproducts with Near-Term Potential*. NREL/TP–5100-65509, 1244312 (OSTI, 2016); http://www.osti.gov/servlets/purl/1244312/; https://doi.org/10.2172/1244312
21. Pointner, M., Kuttner, P. & Obrlik, T. Composition of corncobs as a substrate for fermentation of biofuels. *Agron. Res.* **12**, 391–396 (2014).
22. Cheng, M.-T. et al. Particulate matter characteristics during agricultural waste burning in Taichung City, Taiwan. *J. Hazard. Mater.* **165**, 187–192 (2009).
23. Van Nieuwenhove, I. et al. Biobased resins using lignin and glyoxal. *ACS Sustain. Chem. Eng.* **8**, 18789–18809 (2020).
24. Pickett, D. J. & Yap, K. S. A study of the production of glyoxylic acid by the electrochemical reduction of oxalic acid solutions. *J. Appl. Electrochem.* **4**, 17–23 (1974).
25. Scharbert, B. & Babusiaux, P. Electrochemical process for reducing oxalic acid to glyoxylic acid. US patent US005395488A (1995).
26. Schuler, E., Demetriou, M., Shiju, N. R. & Gruter, G.-J. M. Towards sustainable oxalic acid from CO_2 and biomass. *ChemSusChem* **14**, 3636–3664 (2021).
27. Davis, R. et al. *Process Design and Economics for the Conversion of Lignocellulosic Biomass to Hydrocarbons: Dilute-Acid and Enzymatic Deconstruction of Biomass to Sugars and Catalytic Conversion of Sugars to Hydrocarbons*. NREL/TP–5100-62498, 1176746 (OSTI, 2015); http://www.osti.gov/servlets/purl/1176746/; https://doi.org/10.2172/1176746
28. Motagamwala, A. H. et al. Toward biomass-derived renewable plastics: production of 2,5-furandicarboxylic acid from fructose. *Sci. Adv.* **4**, eaap9722 (2018).
29. Straathof, A. J. J. & Bampouli, A. Potential of commodity chemicals to become bio-based according to maximum yields and petrochemical prices. *Biofuels Bioprod. Biorefining* **11**, 798–810 (2017).
30. Lange, J. & Wyser, Y. Recent innovations in barrier technologies for plastic packaging—a review. *Packag. Technol. Sci.* **16**, 149–158 (2003).
31. George, N. & Kurian, T. Recent developments in the chemical recycling of postconsumer poly(ethylene terephthalate) waste. *Ind. Eng. Chem. Res.* **53**, 14185–14198 (2014).
32. Stloukal, P., Jandikova, G., Koutny, M. & Sedlařík, V. Carbodiimide additive to control hydrolytic stability and biodegradability of PLA. *Polym. Test.* **54**, 19–28 (2016).
33. Sato, H., Akutsu, F., Kobayashi, F. & Okada, Y. Process for producing aliphatic polyester. US patent US7538178B2 (2009).
34. *Glyoxylic acid—Registration Dossier* [online] (ECHA, accessed 29 March 2021); https://echa.europa.eu/registration-dossier/-/registered-dossier/14954/6/2/8
35. *1,4-Butanediol—Registration Dossier* [online] (ECHA, accessed 29 March 2021); https://echa.europa.eu/registration-dossier/-/registered-dossier/15496/1
36. *1,5-Pentanediol—Registration Dossier* [online] (ECHA, accessed 29 March 2021); https://echa.europa.eu/registration-dossier/-/registered-dossier/14818/6/2/8
37. *1,6-Hexanediol—Registration Dossier* [online] (ECHA, accessed 29 March 2021); https://echa.europa.eu/registration-dossier/-/registered-dossier/15109/6/2/1

Methods

The methods for DMGX synthesis both from xylose and lignocellulosic biomass, as well as their subsequent polymerizations to produce polyesters, are briefly described in the main text. More detailed synthesis methods, material descriptions, detailed analytical and material characterization procedures, and life-cycle analysis and technoeconomic analysis methodologies are provided in Supplementary Sections 1 and 2.

Data availability

All data needed to support the findings of this study are included in the main text or in the Supplementary Information. Crystallographic data for the structure reported in this Article have been deposited at the Cambridge Crystallographic Data Centre, under deposition no. CCDC 2121378 (1S-DMGX). Copies of the data can be obtained free of charge via ccdc.cam.ac.uk/structures/Search?ccdc=2121378. All of the data associated with the Article have been deposited[38] with Zenodo at https://zenodo.org/record/6482769.

References

38. https://doi.org/10.5281/zenodo.6482769

Acknowledgements

This work was supported by the Swiss National Science Foundation (grant no. CRSII5_180258) and the National Competence Center Catalysis (grant no. 51NF40_180544), by the European Research Council (ERC) under the European Union's Horizon 2020 research and innovation programme (grant CATACOAT, no. 758653) and under a Marie Skłodowska-Curie grant agreement no. 945363, by the Swiss Competence Center for Energy Research: Biomass for a Swiss Energy Future through the Swiss Commission for Technology and Innovation (grant no. KTI.2014.0116) and by EPFL (partly through the Tech4Dev programme). We thank M. Studer from the Bern University of Applied Sciences (Switzerland) for providing various wood samples, IP-Suisse for providing corn cob samples, C. Wegmann for compositional analyses of the biomass feedstocks, M. Hannebelle and A. Gagliardi for assisting with the vacuum forming, F. Fadaei Tirani for crystal structure determination, S. Bertella for assistance with graphic design and illustrations, L. Blanchard for assistance with TGA measurements and A. Magrez for powder XRD measurements.

Author contributions

L.P.M. and J.S.L. conceived of the project and designed the research. L.P.M. performed most of the experiments and drafting of the manuscript. G.R.D. performed most of the biomass fractionation and lignin upgrading experiments and helped design syntheses. A.D. performed most of the material characterization experiments and was supervised by Y.L. and V.M. M.A.H., with the assistance of C.R., performed the catalyst optimization and some of the polymerization, purification and material characterization experiments. M.J.J. performed the life-cycle analysis, aided with the technoeconomic analysis and was supervised by F.M. T.R. performed the pretreatment experiments on the corn cob feedstock. I.S. performed gel permeation chromatography experiments supervised by A.P. M.V. performed injection moulding and tensile strength testing of the PAX samples. H.-A.K. helped design some of the polymerization and characterization experiments. All authors contributed to editing the manuscript.

Competing interests

The authors declare the following competing financial interests. L.P.M., G.R.D. and J.S.L. are inventors on a European patent application (EP19203000.5) on methods for producing the renewable monomer and polymer described here. G.R.D. and J.S.L. are inventors on a European patent application (EP19202957.7) on methods for producing fragments of lignin with functional groups. J.S.L. is an inventor on a European patent application (EP16165180.7) on methods for producing lignin monomers from lignocellulosic biomass during biomass depolymerization. J.S.L. is a co-founder, and M.A.H. a shareholder, of Bloom Biorenewables Ltd, which is exploring commercial opportunities for aldehyde-stabilized lignin and aldehyde-protected xyloses. The remaining authors declare no competing interests.

Additional information

Extended data is available for this paper at https://doi.org/10.1038/s41557-022-00974-5.

Supplementary information The online version contains supplementary material available at https://doi.org/10.1038/s41557-022-00974-5.

Correspondence and requests for materials should be addressed to Jeremy S. Luterbacher.

Peer review information *Nature Chemistry* thanks the anonymous reviewer(s) for their contribution to the peer review of this work.

1. Aldehyde protection on rotary evaporator
90°C, 40 mbar, 3 hrs

96 %

2. Esterification in 70 wt% methanol
Reflux, 2 hrs

99 %

3. Neutralization with sodium
bicarbonate at 4°C to pH=4

94 %

4. LLE after evaporation of methanol
Add 3 mL DCM/g DMGX and wash 3x with water

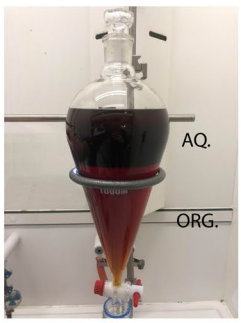

93 %

5. Vacuum-distillation of DCM extract
180°C, 0.1 mbar

95 %

6. Crystallzation of DMGX oil in EtOH
24 mL EtOH/g DMGX at 70°C, cool to -20°C

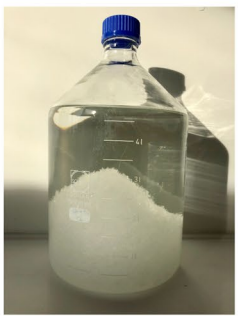

77.4 %

7. Melt condensation of DMGX and diol
190°C, 0.05-0.1 mbar

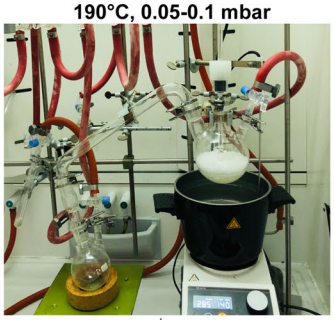

8. Precipitation of polymer
HFIP into IPA

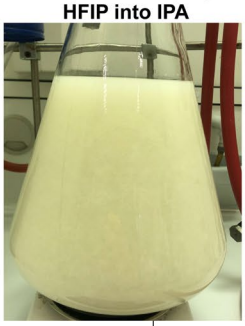

9. Compression-moulded plastic
140°C, 10 kN, 20 min

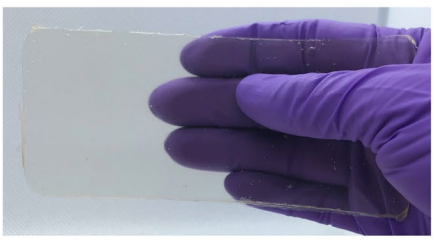

89-96.4 %

Extended Data Fig. 1 | Photos and process yields for production of PAX from commercial xylose. Alternatively, production steps 3–5 can be replaced by directly precipitating DMGX from the crude esterification reaction (see Extended Data Fig. 4).

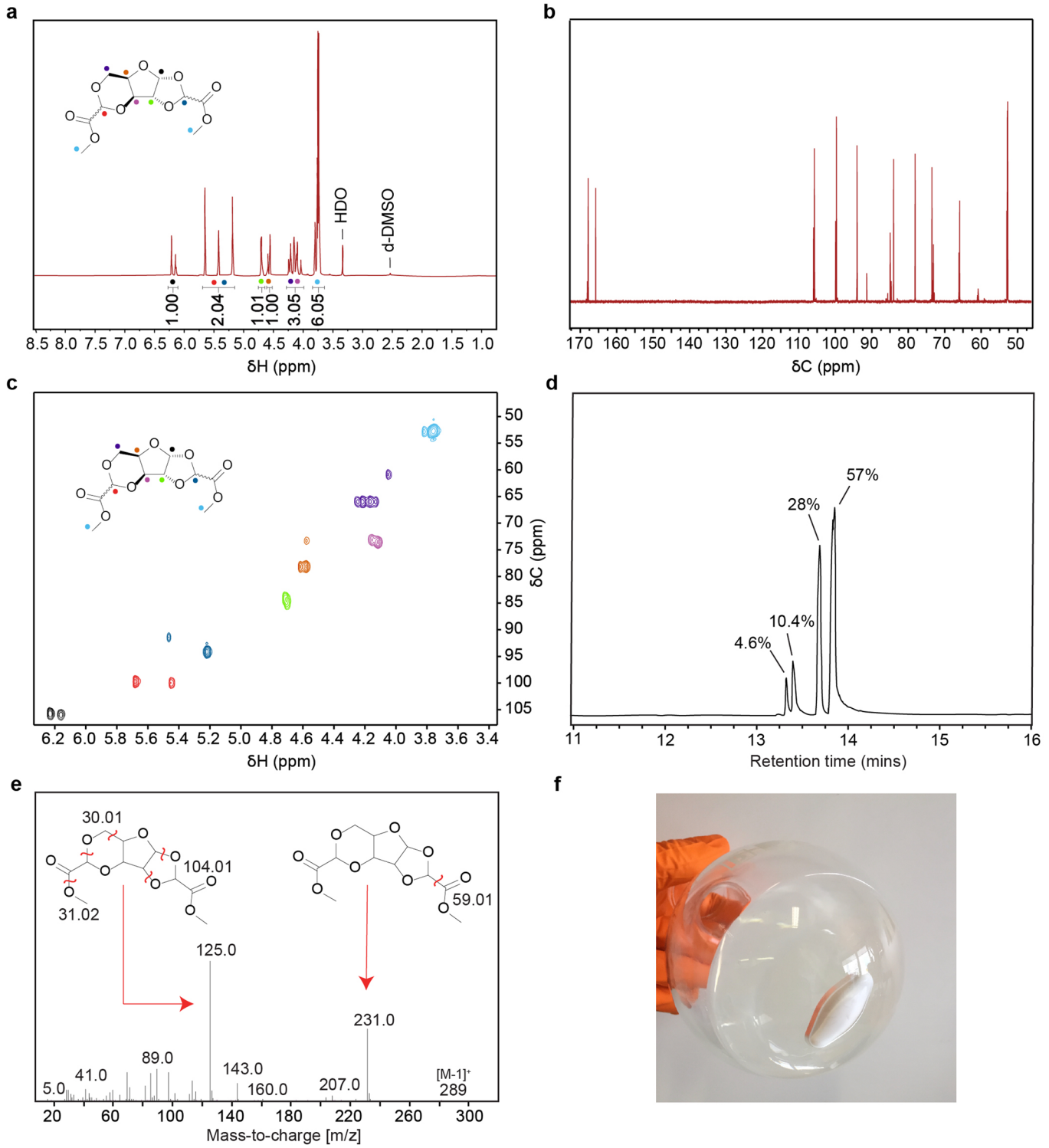

Extended Data Fig. 2 | Characterization of the distilled DMGX (4-stereoisomer oil) used in polymerizations. a, ^{1}H NMR spectrum. **b**, ^{13}C NMR spectrum. **c**, 2D HSQC NMR spectrum. **d**, GC chromatogram with percent abundance of each stereoisomer. **e**, GC-MS spectrum (combination of 4 stereoisomers). **f**, Photo of DMGX 4-stereoisomer oil. NMR spectrums were acquired in DMSO-d_6 at 25 °C.

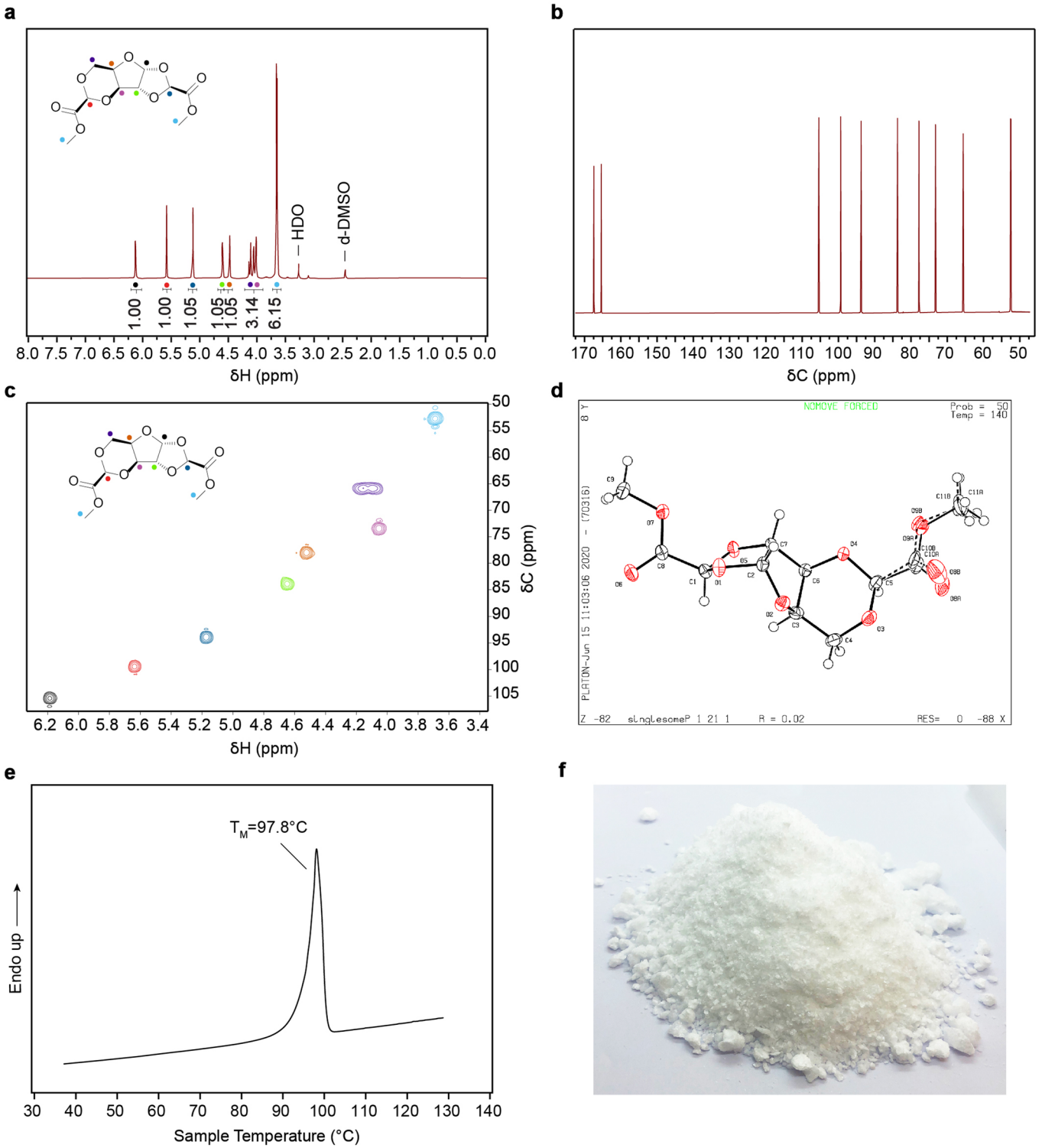

Extended Data Fig. 3 | Characterization of the crystalline DMGX single isomer used in polymerizations. a, ^{1}H NMR spectrum. **b**, ^{13}C NMR spectrum. **c**, 2D HSQC NMR spectrum. **d**, Crystal structure with probability ellipsoids. The structure was submitted to the Cambridge Crystallographic Data Centre (CCDC) with deposition number CCDC 2121378. **e**, DSC curve of crystalline DMGX (melting point was determined by maximum of the 1st derivative of DSC curve). **f**, Photo of DMGX single isomer crystals. NMR spectrums acquired in DMSO-d_6 at 25 °C.

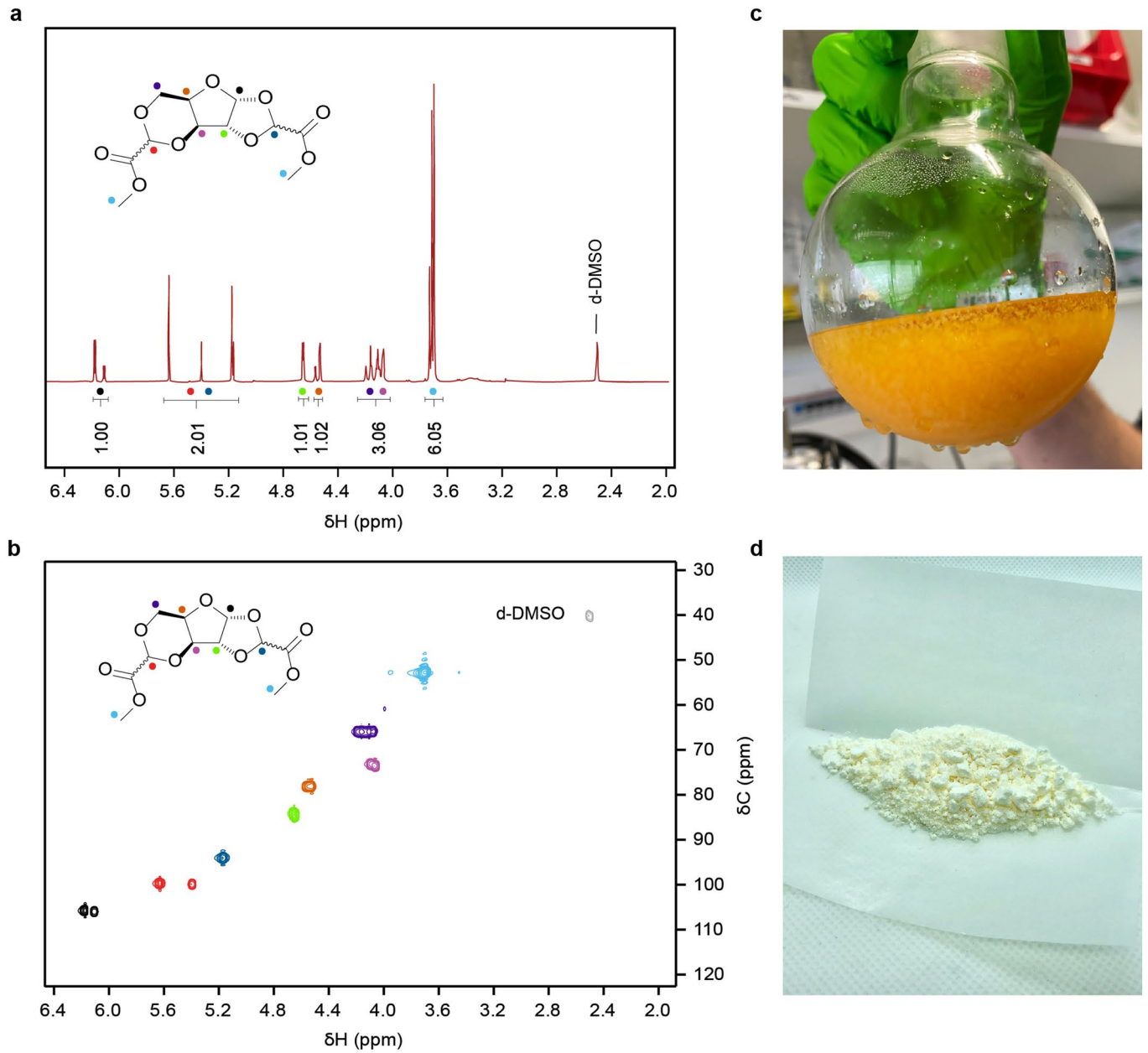

Extended Data Fig. 4 | Recovery of DMGX via direct precipitation from the crude esterification mixture. a, ^{1}H NMR spectrum of the precipitate taken in DMSO-d_6 at 25 °C. **b**, HSQC NMR spectrum of the precipitate taken in DMSO-d_6 at 25 °C. **c**, Photo of **DMGX** precipitating from esterification mixture after chilling the mixture on ice. **d**, Photo of the precipitate after filtration from the mixture.

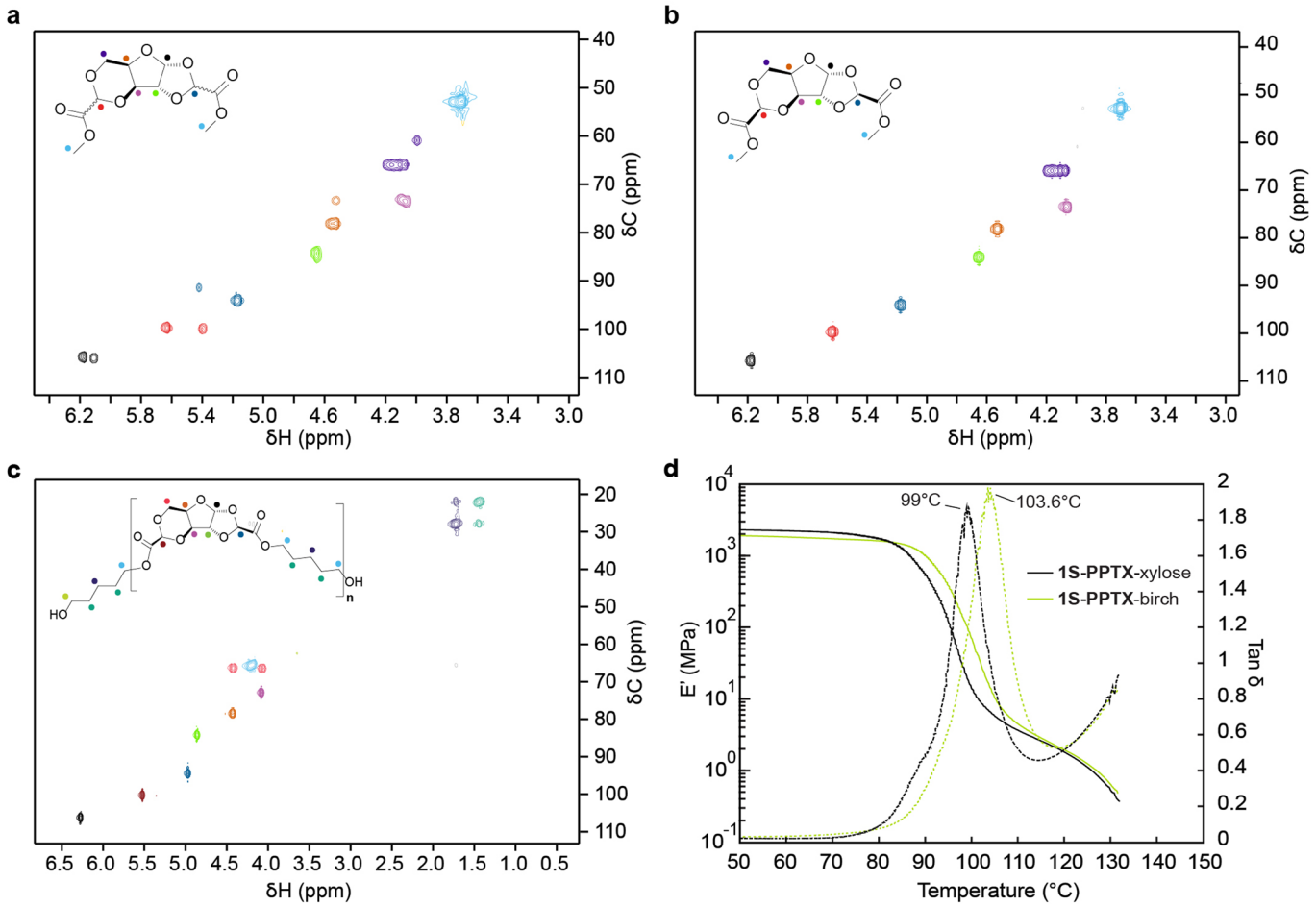

Extended Data Fig. 5 | DMGX and PAX derived from lignocellulosic biomass. a, 2D HSQC NMR of distilled DMGX produced from birch wood taken in DMSO-d_6 at 25 °C. **b**, 2D HSQC NMR of crystalline DMGX single isomer produced from birch wood taken in $CDCl_3$ at 25 °C. **c**, 2D HSQC NMR of 1S-PPTX produced using DMGX from birch wood taken in $CDCl_3$ at 25 °C. **d**, DMA curves of 1S-PPTX polymers derived from xylose and from birch wood. Tan delta curves are dashed lines.

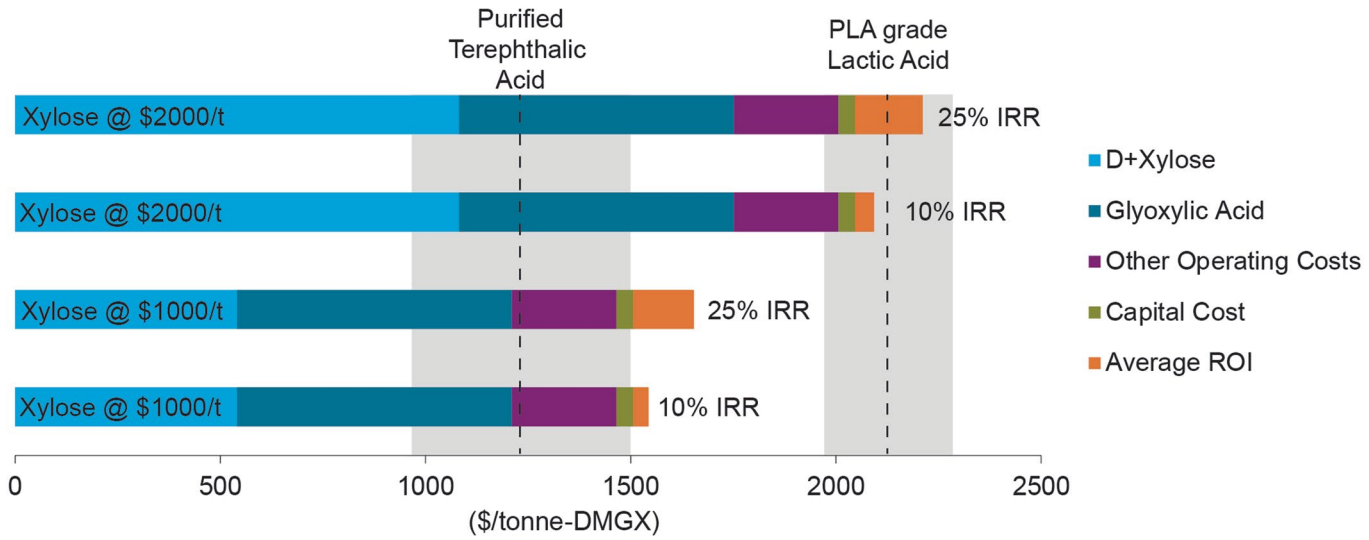

Extended Data Fig. 6 | Minimum selling price of DMGX produced from commercial xylose under various economic scenarios. Black dashed lines are mean prices for purified terephthalic acid and PLA grade lactic acid and shaded grey areas represent price ranges. IRR is internal rate of return.

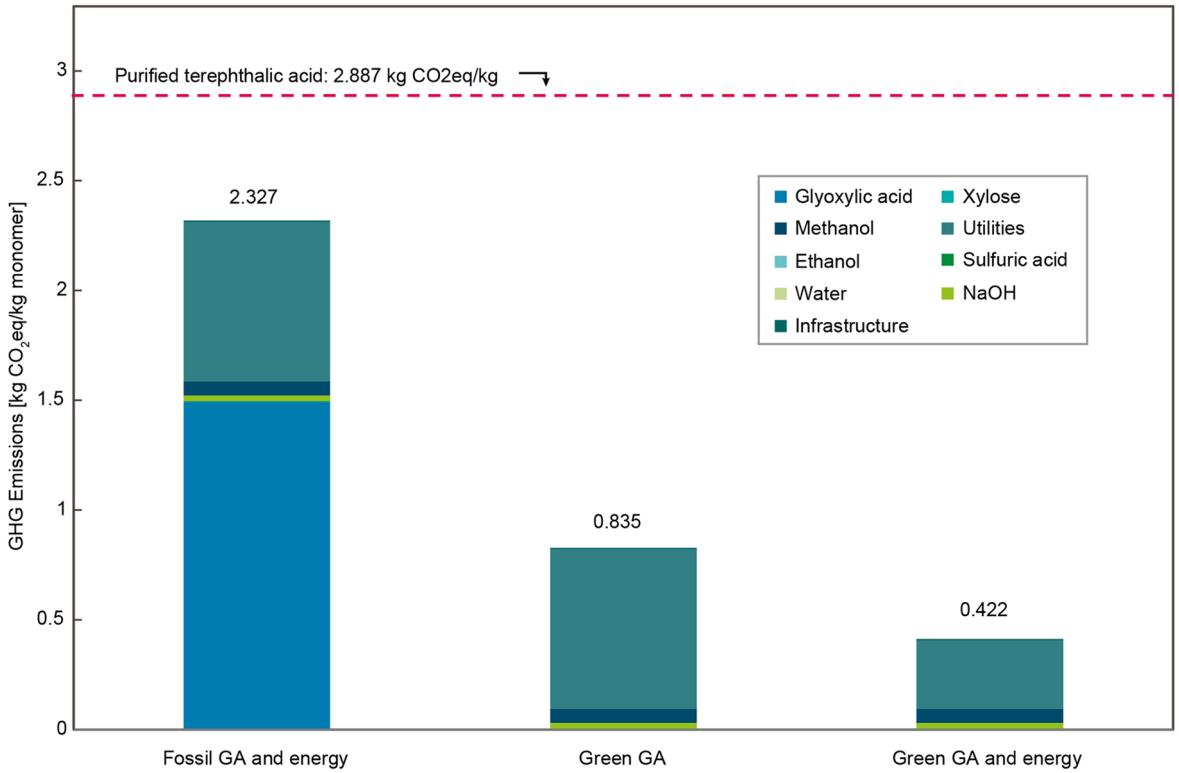

Extended Data Fig. 7 | Global warming potential of DGMX with various carbon sourcing scenarios. (left) Using fossil based glyoxylic acid and natural gas heat and power, (middle) using glyoxylic acid from CO_2 and natural gas heat and power, and (right) glyoxylic acid from CO_2 with biomass burned for heat and power. The red dotted line corresponds to our calculated GWP of commercially available fossil-based purified terephthalic acid.

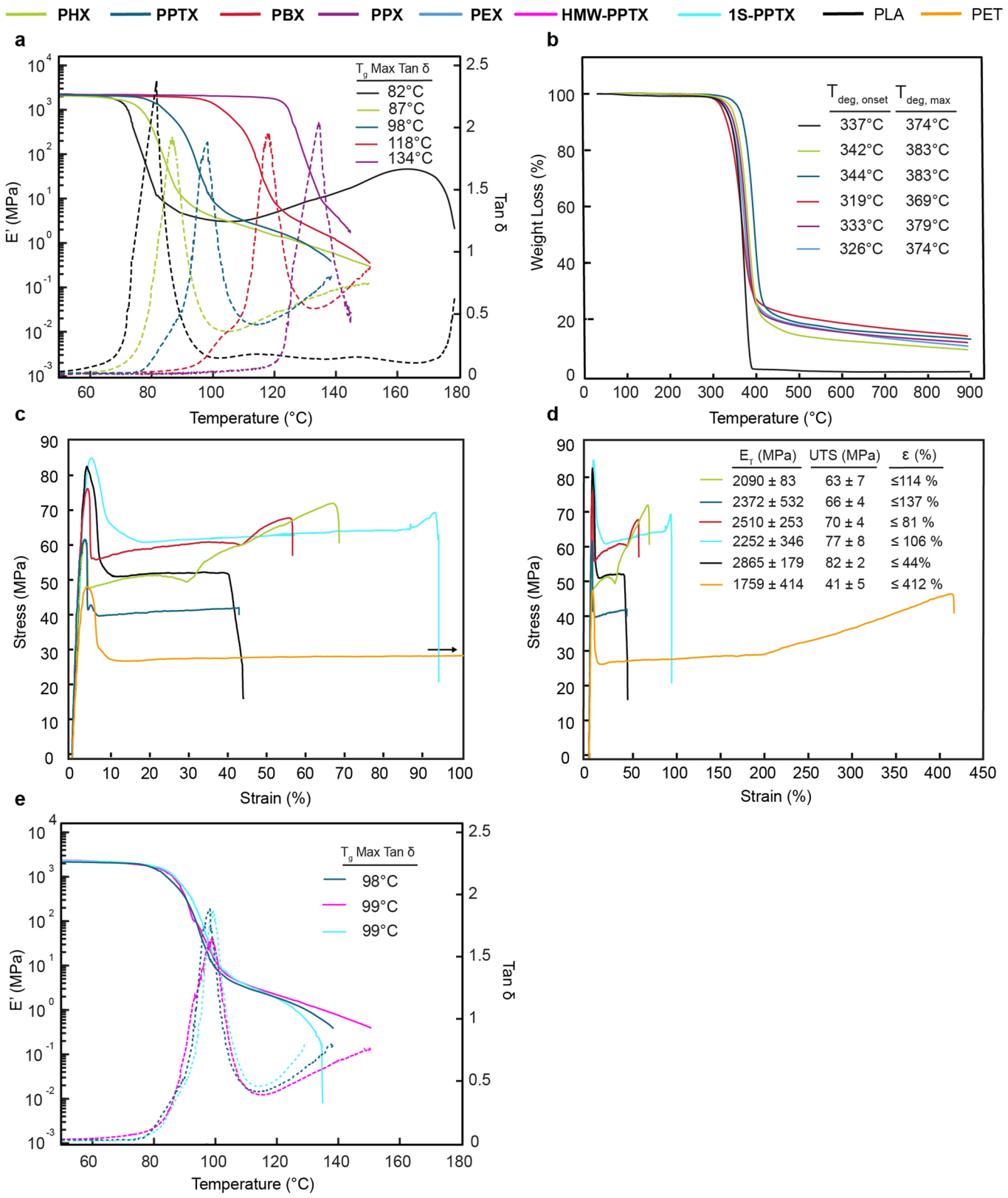

Extended Data Fig. 8 | Supplemental properties of PAX polymers. a, DMA curves for PAX polymers and PLA with heating ramps applied at 3 °C/min from -50 to 200 °C (shown from 50 °C). Tan delta curves are dashed lines. **b**, TGA curves with heating rate of 10 °C/min under nitrogen. Incomplete degradation of PAX polymers is attributed to the cyclic nature of the DMGX monomer which likely leads to formation of non-volatile chars in pyrolysis conditions. **c**, Stress-strain curves of injection-moulded PAX dog bone samples with PLA (NatureWorks 4032D) and PET (Terez 3200) curves for comparison. The displayed curves are from single representative samples but reported tensile data values are all averages of 3–5 samples. **d**, Full version of panel C with tabulated tensile values. **e**, DMA curves for pentanediol-based polymers with heating ramps applied at 3 °C/min from −50 to 200 °C (shown from 50 °C). Tan delta curves are dashed lines.

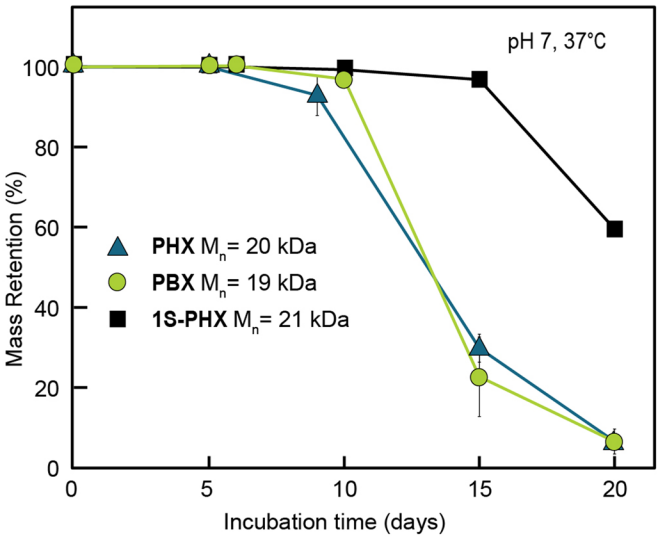

Extended Data Fig. 9 | Hydrolytic stability of various PAX polymers in pH 7 phosphate buffer at 37 °C. The hydrolytic studies were performed in the same manner as detailed in the Supplementary Information section 1.7.14. All polymer films had an initial starting number average molecular weight (M_n) of ~20 kDa. These experiments were performed in triplicate. Error bars represent standard errors.

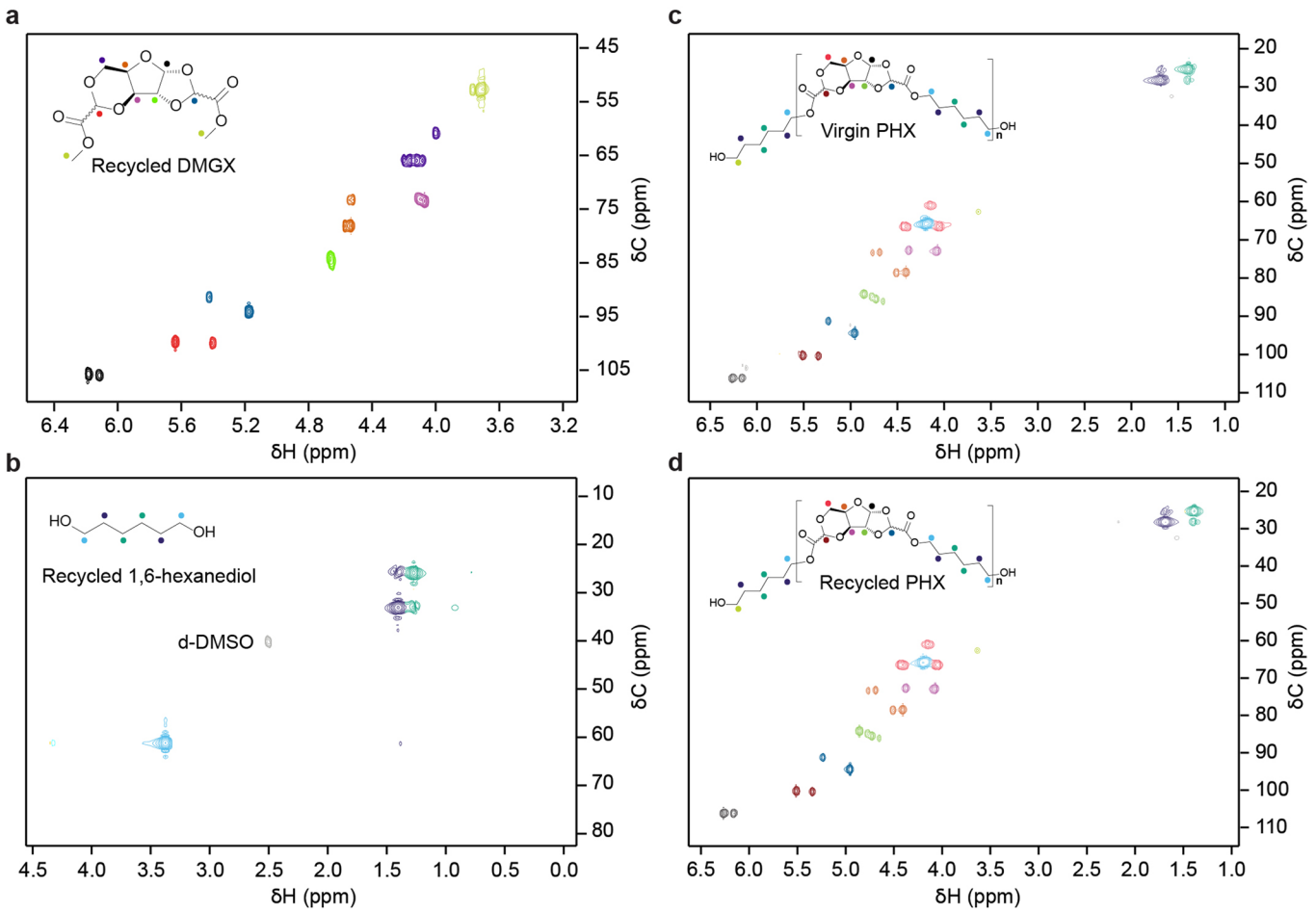

Extended Data Fig. 10 | 2D HSQC NMR spectra of chemically-recycled monomers and plastic. a, Recycled DMGX. **b**, Recycled 1,6-hexanediol. **c**, Original PHX used for chemical-recycling study. **d**, The final recycled PHX using the recycled DMGX and 1,6-hexanediol. NMRs were taken in *d*-DMSO at 25 °C for the monomers and $CDCl_3$ at 25 °C for the polymers.